Conducting a Comprehensive Physical Investigation on Uncontrolled Internal Soil Erosion Leading to Sinkholes in Anambra State, Nigeria

Abstract:

Uncontrolled infiltration of water poses a significant environmental threat, capable of causing severe damage to structures and farmland if left unaddressed. In the context of Anambra state, Nigeria, uncontrolled infiltration has emerged as the primary cause of internal erosion, leading to the formation of numerous sinkholes scattered throughout the region. Consequently, this study aimed to analyse the physical dynamics of the soils surrounding these sinkholes within the state. The investigation was conducted across three distinct locations: Awka site 1 (6.2232°N and 7.0824°E), Awka site 2 (6.2220°N and 7.0819°E), and Agulu (6.3401°N and 7.1233°E). A total of 24 soil samples were collected and analysed, comprising of 15 samples from the immediate vicinity of the sinkholes and 9 samples obtained from areas located at least 2Km or more from the sinkholes. The parameters examined included pH, Electrical Conductivity (EC), Total Dissolved Solids (TDS), Organic Carbon (OC), Organic Matter (OM), erodibility Factor (K), Moisture Content (MC), Bulk Density, Total Porosity and soil texture. The results revealed a range of pH values, with the piping zone exhibiting a pH of 5 and below, while the non-piping zone predominantly displayed a pH of 6 and above. This discrepancy indicates soil sodicity, suggesting potential challenges in terms of soil quality. Furthermore, the electrical conductivity values varied from 2.21 to 7.21 μS/cm, signifying differing levels of ion concentration within the examined areas. Additionally, the analyses indicated a substantial depletion of organic content, with the piping zone registering a meager organic content value of 2.43. Investigations of soil texture within the piping regions highlighted a notably low clay content, ranging from 2.5% to 6.7%. This finding suggested that significant drainage of the soil has potentially influenced the overall soil stability and the observations underscoring the presence of dispersive processes within the soil, further contribute to the prevailing conditions.
Keywords: Infiltration, Internal erosion, Sinkholes, Soil piping, Dispersion, Sodicity, Anambra state.

Introduction

The movement of water through soil pores, known as infiltration, enables various processes such as nutrient absorption by plants[1]–[3], groundwater recharge[4], and the accumulation of liquid minerals[1]. Infiltration depends on multiple factors, including soil permeability, pressure gradient, gravitational force, and the velocity of flowing water[1], [3], [5], [6]. Monitoring the velocity of infiltration is crucial for maintaining the chemical balance and elastic properties of the soil[3], [7]. Low infiltration velocity is often identified as the primary cause of internal erosion, which happens when water gradually carries away fine particles within the coarse soil matrix[6], [8], [9].

Internal erosion, commonly referred to as soil piping[10]–[13], is a phenomenon that can occur in any geographical setting[6], [14]–[16]. Through extensive research and observations, researchers have found evidence of soil piping in a wide range of soil types, such as duplex[17], [18], loess[18], [19], and uniform clay soils[15]. It should be noted that soil piping failures have been witnessed not only in impermeable soils, but also in highly permeable ones that contain expansive clays like montmorillonite and kaolinite[14], [20]. Additionally, the occurrence of soil piping has been observed across diverse climatic regions, characterized by variations in temperature, rainfall, and the seasonal patterns of rainfall[15], [21]. These findings emphasize the significance of understanding and addressing soil piping as a potential geotechnical concern in various locations and soil conditions.

The complex nature of piping, which has been extensively studied, comes as a result of a multifaceted interplay between physical and chemical processes, often associated with mechanical scouring, entrainment, or mass wasting [15]. These processes can lead to significant environmental transformations and unconventional rainfall patterns [22]. It is worth

noting that human activities have been identified as significant contributors to the development of piping erosion worldwide [17], [23].

Human interference can be categorized into two main groups: those affecting soil stability and those influencing the local water balance. Clearing land for agriculture, overgrazing, irrigation, and construction works are among the commonly cited activities that have detrimental effects on soil stability [23], [24]. Vegetation loss and livestock trampling result in reduced soil protection, leading to a decrease in soil quantity [24]. This reduction in soil quantity subsequently lowers the infiltration rate [22], [25]. Such changes can be attributed to alterations in soil chemical properties, which often result in structural instability, including clay dispersion and the development of a thin surface seal [22], [26].

Consequently, a decrease in the infiltration rate allows precipitation to generate runoff, carrying soil and other particles. The interaction between these particles during transport, including mechanical scouring, can lead to the creation of holes in the soil, ultimately causing piping and changing the local water balance [27]–[29]. These findings underline the importance of recognizing the role of human activities and their impact on soil stability, water balance, and the subsequent development of piping erosion.

When rainwater interacts with bare soil, several processes come into play [22], [28], [29]. The impact energy of raindrop compacts the soil surface and contributes to enhanced dispersion [28], [29]. Moreover, rainwater carries electrolytes that increase the soil solution, affecting soil stability by elevating the salt or sodium content [22], [30]. In certain areas, the presence of sodium can lead to the deterioration of soil structure, resulting in soil dispersion. It is important to note that when a dispersive soil contains more than 6.0% exchangeable sodium (ESP), it becomes prone to piping phenomena [22], [25], [31].

Dispersive soil solutions can be identified by assessing their pH and Electrical Conductivity (EC) values [22], [25], [31]. The pH of soil is a measure of the activity of hydrogen ions and is influenced by the relative amounts of absorbed hydrogen and metallic ions. It provides valuable information about soil properties such as phosphorous availability and base status. In the case of soils prone to soil piping, their pH values typically fall within the range of 5 to 8, resembling those of sodic soils [24], [25].

Electrical conductivity, on the other hand, quantifies the ability of a soil-water mixture to conduct an electrical current. It depends on the total concentration of ionized substances dissolved in the soil-water mixture [8], [32]. In the context of soil, the focus has primarily been on the impact of Exchangeable Sodium Percentage (ESP) and electrolyte concentration (EC) on excessive swelling, dispersion, hydraulic conductivity, and crust formation during drying [25]. When relatively low EC water percolates through potentially dispersive soils, the leaching of salts from the soil profile may trigger spontaneous dispersion, resulting in the formation of tunnels [24], [25].

Therefore, according to [33], the practical approach to preventing tunnel development is to divert water away from the catchment areas of these tunnels and emphasizes the importance of understanding and managing pH levels, electrical conductivity, and the leaching of salts to mitigate the risks associated with soil piping and tunnel formation.

Soil piping is not an instantaneous or sudden process; rather, it occurs gradually over time, influenced by the specific characteristics of the area and the type of soil present [34], quoted by [35] identified two preconditions necessary for the formation of piping erosion. Firstly, the soil must disperse into the water that flows through it, allowing the movement of dispersed clay particles. Secondly, either the soil must possess sufficient permeability in the soil matrix or macropores to facilitate the unobstructed movement of these clay particles.

Several physical properties contribute to the occurrence of piping. These include the slope and elevation of the land, the rate of underground water flow, the structure, texture, porosity, and permeability of the erodible material [15], [29], [31], [36], [37]. Additionally, the chemical properties of the soil, such as clay mineralogy, pH levels, presence of sodic soils, and the electrical conductivity of the soil, also play a role in favoring piping[22], [30], [35].

It is important to note that all these factors need to align favorably to initiate soil erosion and piping. If any of these factors are not conducive, the soil may not erode, and piping may not occur [25] quoting [34]. Understanding the interplay between these physical and chemical properties is crucial for comprehending the potential occurrence of soil piping in a given area.

Over the course of several decades, Anambra State in Nigeria has been plagued by numerous cases of soil piping, particularly during periods of high rainfall [38]–[40]. This phenomenon has had significant repercussions for the local communities, with reports indicating that farmlands often become inaccessible, residential structures face foundation threats, and movement is hindered due to the collapse of pathways [41], [42]. The researchers have witnessed firsthand the detrimental effects of soil piping on the lives of the people in this region.

Despite the government and other stakeholders in the state investing substantial financial resources in combating this issue, progress has been limited. Various methods, including the use of cover-ups, have been employed, but success has been elusive. It is evident that a more comprehensive understanding of the causes of soil piping is needed to effectively address this challenge.

In light of this, our study aims to analyze the physico-chemical characteristics of dispersive soils that have contributed to the natural occurrence of sinkholes in three erosion-prone areas within Anambra State. By delving deeper into the underlying causes of soil piping, we hope to gain valuable insights that can inform more targeted and effective strategies for mitigating this phenomenon.

Study Area

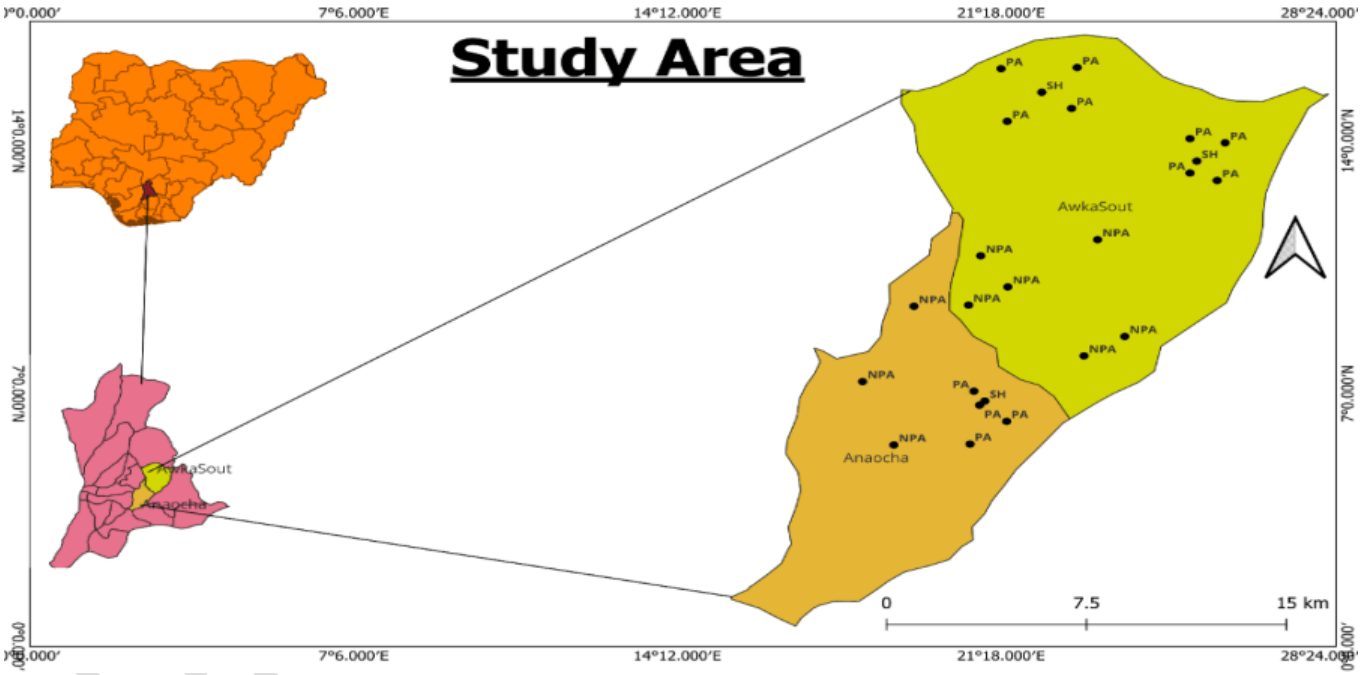

Figure 1. The study area with an insert of Anambra state and Nigeria (SH = Sinkholes, PA = Piping Area, NPA = Non-piping area)

In this study, our focus is on two specific sites within the Awka South area and one site in the Aniocha Local Government area of Anambra State, Nigeria (as shown in Figure 1). The first site, Awka Site 1, is situated at coordinates (6.2232°N and 7.0824°E). Here, a soil pipe with a diameter of approximately 5 cm has caused significant damage to a constructed road. This damage has resulted in the formation of double sinkholes, each with a diameter of around 70 cm (refer to Figure 2a).

The Awka Site 2, located at coordinates (6.222°N and 7.0819°E), we find a soil pipe that has been present for approximately three years. This pipe has caused the formation of multiple holes, each with an average diameter of 10 cm, as well as a visible sinkhole measuring around 100 cm in diameter (as depicted in Figure 2b).

Lastly, our third site is situated in Agulu, with geographical coordinates (6.3401°N and 7.1233°E). By closely examining these three sites, we aim to gain a deeper understanding of the characteristics and formation mechanisms of soil pipes in areas prone to sinkholes.

Figure 2. (a) Sinkhole at Awka site 1 (b) Soil pipe at Awka site 2

Geology and Global Information System of Anambra state

Anambra State, located in the southern part of Nigeria, occupies a geographical area of latitude 5.7503°N and 6.7503°N, and longitude 7.2502°'E and 7.7502°E. It is an integral part of the Anambra Sedimentary Basin, which is situated in the southern region of Nigeria (as illustrated in figure 3a). The state covers an expansive area of approximately 40,000 square kilometers, as documented by [43]and [44].

The southern boundary of the Anambra Basin aligns with the delta swamps of the Niger Delta Basin, extending northwards beyond the Bende Ameki Formation [45], [46]. It is widely believed that the formation of the basin occurred concurrently with the folding and uplift of the Abakaliki-Benue area during the Santonian era [47]. Consequently, the Anambra Basin serves as a significant center for the deposition of clastic deposits and deltaic sequences [47]. These formations are a result of tectonic activity within the second Lower Benue Trough, which played a crucial role in the geological evolution of the area (see figure 3a) [45].

Anambra basin boasts of a geological composition that is rich in ancient Cretaceous delta deposits, constituting the sedimentary rocks found within the region. The basin is predominantly characterized by the Nnaka Sand, which dates back to the Ecocene period [45], [47]. Overlying this sandy formation is the paralic Ogwashi-Asaba formation, originating from the Oligocene epoch. On the other hand, the marine Imo shale underlies a significant portion of the basin [47].

It is worth noting that the presence of these sands, primarily the coastal plain sands, has contributed to ecological challenges in the area. These sands exhibit a high susceptibility to erosion, leading to severe ecological problems within the region. Underneath the weak lateritic and acidic soils lie unstable and poorly consolidated geological rocks and materials [46], [47]. The sandy components of these geological units house substantial groundwater reservoirs, known as aquifers [44]. However, these aquifers pose a threat when subjected to excessive pore water pressures, especially when overlying structures bear uncompromising loads [43].

In addition to these geological characteristics, the lateritic and sandy soils are highly vulnerable to erosion caused by storm water runoff. This erosion can further exacerbate the ecological issues faced by the region.

The state has a distinctive topography characterized by rugged reliefs and uplands (see Figure 3b) [48]. The study area itself is situated entirely within the Awka-Orlu upland [48]. The state is generally well drained, except for the northern parts, which experience poor drainage conditions and are highly susceptible to flooding (see Figure 3c).

The intricate network of rivers, lakes, and tributaries, along with their groundwater components, is distributed throughout the state in a manner that significantly influences the formation, development, and dynamics of erosions and landslides. These natural water bodies and their flow patterns play a crucial role in shaping the landscape of Anambra State.

The primary drainage system for the state is the Anambra River, which ultimately empties into the mighty River Niger. Additionally, numerous tributaries can be found at various locations, effectively draining the state. Of notable mention is the Agulu Lake, which serves as the closest natural drainage system to the study area.

Anambra State experiences a climate typical of the tropical rainforest zone. The climate is characterized by two distinct seasons: the rainy season, which follows a conventional pattern from April to October, and the dry season, spanning from November to March. During the rainy season, the state receives an average precipitation of 602mm [48].

One noteworthy weather phenomenon during the mid-dry season is the intrusion of a strong dry wind known as the Harmattan, originating from the northern region of the country. This wind engulfs the entire state and contributes to the drying out of the soil, resulting in caking. The Harmattan wind poses challenges to agricultural activities and soil moisture retention in Anambra State [49]. Temperature variations are also prominent in the region. During the harsh dry season, temperatures can soar as high as 35°C, while in the rainy season, they tend to be more moderate, reaching as low as 18°C [49] (see Figure 3d).

From analyzes the records of land cover in Anambra State, it becomes evident that the region has experienced significant loss of its natural land cover and an increase in bare lands due to the expansion of built-up areas (see Figure 3e). This phenomenon is particularly pronounced in the central and western parts of the state, where the concentration of built-up areas has grown larger and more aggregated over time[48].

Consequently, there has been a considerable increase in Land Surface Temperature (LST) across the state. The LST trends reveal that the central and western parts of Anambra State exhibit higher temperatures compared to the outlying areas of the northern and southern regions (see Figure 3f). This spatial variation in LST can be attributed to the intensified urbanization and subsequent loss of vegetal land cover in the state [48].

The loss of vegetal land cover due to urbanization has several negative consequences. Firstly, it contributes to the elevated Land Surface Temperature and aggravating the already poor condition of the soil. Secondly, the absence of vegetal cover reduces erosion resistance, further exacerbating the vulnerability of the soil to erosion processes.

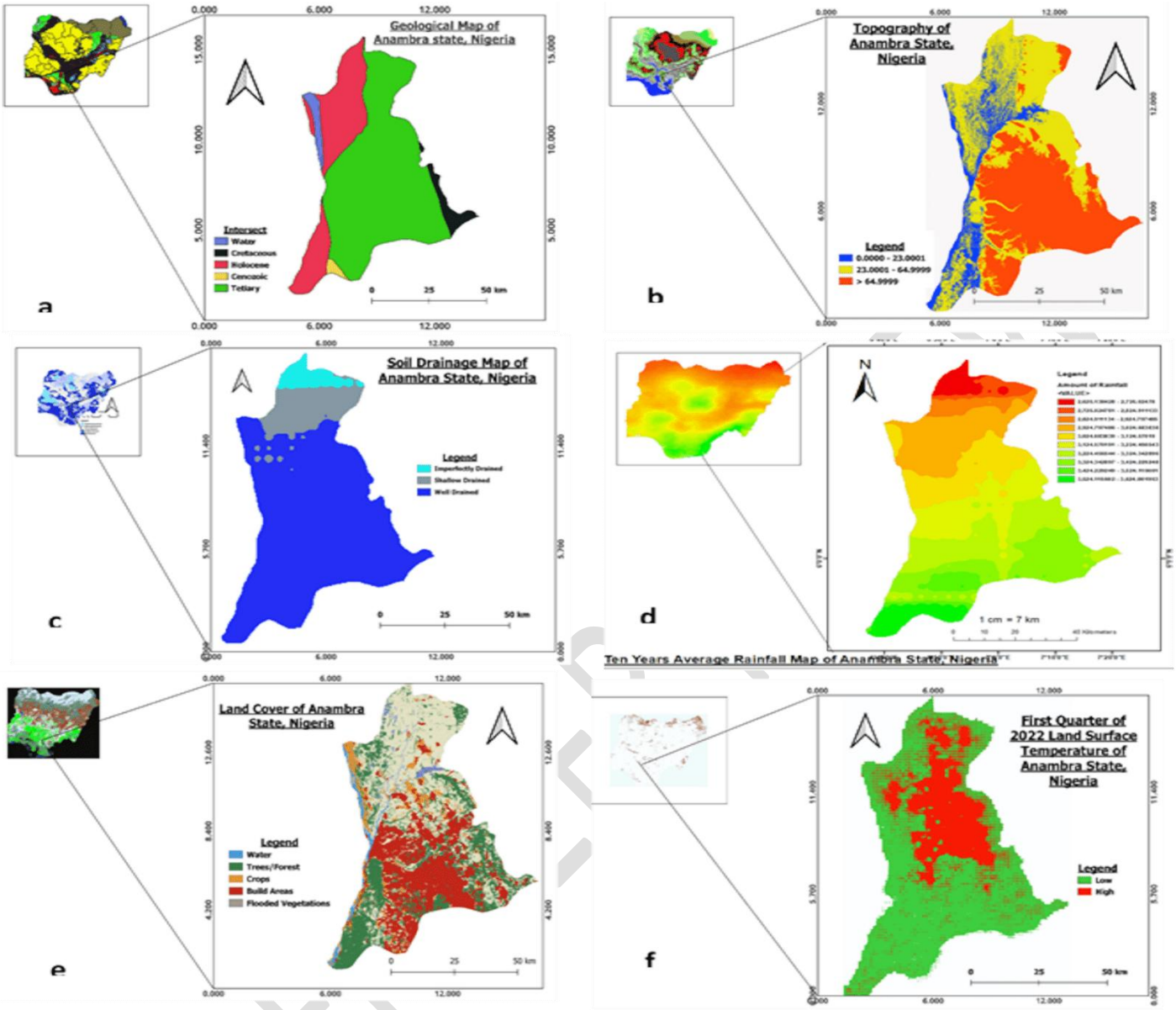

Figure 3 (a) Geological map of Anambra state (b) Topography map of Anambra state (c) Soil drainage map of Anambra state (d) 10 years average rainfall of Anambra state (e) Land cover map of Anambra state (f) First quarter of 2022 land surface temperature map of Anambra state

Materials

To conduct this research, the following materials were utilized: auger, spade, container for soil samples, refrigerator (for sample storage), oven (for drying sampled soils), pestle, a 2mm and 0.5mm mesh sieves for soil sieving, weighing balance.

The parameters examined in this study include pH, Electrical Conductivity (EC), Total Dissolved Solids (TDS), Organic Carbon (OC), Organic Matter (OM), erodibility Factor (K_f), Moisture Content (MC), Bulk Density (D_B), Total Porosity (P_t) and soil texture.

Method

In order to determine the values of the various parameters mentioned above, 24 soil samples were collected from both sinkhole-affected localities and unaffected sections of the study area. The samples were taken at a depth of 0-5ft. Specifically, 15 samples were collected from the piping area (PA) with sinkholes (SH), and 9 samples were collected approximately 2Km away from a known piping area (non-piping area, NPA). The locations where each samples were gotten are labeled using alphabetic notations: A1 – A5 are site within the sinkhole vicinity in Awka site 1, A6 – A8 are sit far from the sinkhole, B1 – B5 are site at Awka site 2, within the sinkhole vicinity while B6 – B8 are distance site from the sinkhole. The alphabet C is used to denote the same approach for the Agulu site.

Analysis of Soil Samples

The following steps were taken to analyze the soil samples:

1. Soil samples were spread in a petri dish and dried in an oven at 105°C for a duration of 4 hours.

2. The dried soil samples were then ground and passed through a 2mm mesh aluminum sieve. Soil samples smaller than 2mm were stored in polythene bags for subsequent analysis.

3. The pH values of the soil samples were determined using the procedure outlined by [50]. 20g of soil was added to a 50mL beaker, followed by the addition of 20mL of distilled water. The suspension was stirred for 5 minutes and then allowed to settle for 1 hour to enable the clay particles to settle. The pH readings were obtained using a Mettler Toledo Seven Easy pH Meter.

4. For the measurement of Electrical Conductivity (EC), the prepared dried samples were weighed and placed in labeled containers. 20mL of distilled water was added to each container, and the solution was vigorously stirred to aid the release of acidity from the soil micelles, resulting in a homogeneous solution. An EC meter was then inserted into a clean, dry beaker to determine the EC value. The TDS value was obtained by replacing the EC meter with a TDS meter and recording the corresponding readings.

5. The values of soil organic carbon and organic matter were determined using the Walkey-Black method [50]. The prepared dried samples were further sieved, and 1g of the 0.5mm sample fraction was weighed and transferred into a conical flask. A measured amount of potassium dichromate (K2Cr2O7) and sulfuric acid (H2SO2) were added to the sample, resulting in an exothermic reaction. The solutions, one with the soil sample and one without, were allowed to cool in a ventilated environment. Subsequently, 100mL of distilled water was added to each solution, generating heat. The cooled samples were titrated using three drops of ferroin as an indicator against Ferrous Sulphate solution until a maroon color end-point was observed. A blank titration was conducted at the beginning without the soil solution. The equation (1) and (2), shows the mathematical process.

$$\%Organic\ Carbon = \frac{10(B - T)}{B \times 0.03 \times 100s} \quad (1)$$

B = titre value of blank sample in mL.
T = titre sample for soil sample in mL.
S = weight of soil in gram

$$\%Organic\ Matter = \%Organic\ Carbon \times 1.729 \quad (2)$$

6. For the value of soil moisture content, the weight of the wet the soil content and container were gotten using the gravimetric method. The weight in which the sample was to be placed and the sample were oven dried for 24 hours separately. The weight of the container and the weight of the container when the sample was placed in it were measured respectively. The water content of the soil (ω) is obtained using the relation in equation (3) below.

$$\%\omega = \frac{W_2 - W_3}{W_3 - W_1} \quad (3)$$

W_1= Weight of container

W_2= weight of container + weight of moist soil
W_3 = weight of container + weight of dry soil

7. For the particle size analysis, the Bouyoucous Hydrometer method of [50] was used to determine particle size distribution. The dried sieved 2mm soil samples were weighed and transfer into a beaker. Each soil sample received a calgon solution (sodium hexametaphosphate) that was left to spread and penetrate the samples for 24 hours. The dispersed calgon oiled samples were moved into a 1000mL measuring cylinder and filled with 950mL of distilled water. The soil hydrometer and thermometer were used to take the first reading after each 40 seconds to obtain $H_1$and T_1. The measuring cylinder containing the soil mixture was allowed to stand for 2 hours to determine H_2 and T_2. The particle size distribution was then calculated using equation 4 - 6

$$\%sand = 100 - (H_1 + 0.2(T_1 - 68) - 2)2 \quad (4)$$

$$\%clay = (H_2 + 0.2(T_1 - 68) - 2)2 \quad (5)$$

$$\%silt = 100 - (\%clay + \%sand) \quad (6)$$

8. The erodibility factor was determined by computing the results from the soil particle sizes and organic matter in the equation below [51]. Table 1 and table 2 show the standard erodibility indices of the soil, which were used as guide for the calculation (equation 7) for this research.

$$K_f = \frac{2.173\times10^{-4}(12-OM)\times M^{1.14}+3.25(S-2)+25(P-3)}{100} \quad (7)$$

S = soil structure class (table 1), P = permeability class (table 2)

9. Bulk density, an indication of soil compaction was determined using the core method analysis of Anderson and Ingram [*]. Total porosity, which is the percentage of bulk volume of soil not occupied on the study area, was calculated from the bulk density using the formula in equation (8) below [51].

$$P_t = 100(1 - D_B/D_P) \quad (8)$$

D_p = Particle density assumed to be 2.65g/cm^3 [52].

Table 1. Structural Class Indices of Soil [52]

Soil Structure	Class Index
Very fine granular (<1mm)	1
Fine granular (1 – 2mm)	2
Medium or coarse granular (2 – 5mm)	3
Massive (blocky, platy, columnar, primitive)	4

Table 2 Permeability Code of soil [53]

Permeability Type (cm/h)	permeability Code

Very slow infiltration(<0.125)	6
Slow infiltration (0.125 – 0.5)	5
Slow to moderate infiltration (0.5 – 2)	4
Moderate infiltration (2 – 6.25)	3
Moderate to rapid infiltration (6.25 – 12.5)	2
Rapid infiltration (> 12.5)	1

Results

The results, as depicted in Table 3, Figure 4a, and Figure 4b, show the soil textures analyzed at various depths from the surface of the study area. Upon examination, it becomes evident that both the piping areas and the non-piping areas exhibit a predominant sandy composition. The mean value of sand content ranges between 69.7% and 81.2%. Additionally, the analysis reveals the presence of an low amount of silt soils, with a mean value that ranges from 1.3% to 6.4%,. Furthermore, a considerably low amount of clay soils 14.8% to 24.2%, ranging from was also observed. Remarkably, the highest percentage of sandy soil, amounting to 81.2%, was recorded in location A2 within the piping region and the lowest percentage of clay soil, measuring 1.3%, was found at location C3, also situated in the piping region. Both of these locations are of particular interest due to their association with the investigated sinkholes.

From the soil textural analysis, figure 5b shows that the soil in the study area falls within sandy loam for area located particularly on the non-piping sides of the research area. The loam sandy, sandy loam and sandy clay loam characterized the textural class of the piping region (see figure 5a).

The results, as depicted in Table 4, Figure 4c, and Figure 4d, indicate that the mean value of organic carbon at various depths from the surface of the study area ranges from 0.15% to 0.83%. Notably, the highest concentration of organic carbon was observed at location C6, which belongs to a non-piping region. Conversely, the lowest concentration of organic carbon was found at location A2, which is situated in a piping region. Similarly, the mean value of organic matter at different depths also ranges from 0.26% to 0.83%, and the highest and lowest values of organic matter align with those of organic carbon. This correlation arises from the direct derivation of organic matter values from organic carbon measurements. For the erodibility factor, the mean distribution across the different analyzed depths in the study area ranges from 0.1 to 0.35. The highest and lowest values of the erodibility factor were observed in the piping region.

Examining the moisture content, as depicted in Table 5, Figures 4e, and 4f, the total mean values at different depths range from 4.45% (observed at location A1, a sinkhole) to 15.08% (found at location A8, a non-piping region). The bulk density, which serves as an indicator of soil compaction, shows a mean values range from 1.51 g/cm^3 to 1.63 g/cm^3. The highest bulk density value was recorded at locations A1 and A2, a piping region, while the lowest value was observed at locations B7, B8 and C8, the non-piping regions. Lastly, the average total porosity at different depths within the study area ranges from 37.18% (noted at location A1, the sinkhole) to 41.92% (observed at location B8, a non-piping region) [1].

The mean values of soil pH at different depths within the study area range from 4.3 to 7.2, as indicated in Table 6, Figures 4g, and 4h. This range can be described as ranging from acidic to alkaline. Notably, the highest and lowest pH values were observed at location A1, which is a sinkhole, and location A8, a non-piping region, respectively. For the electric conductivity, the average distribution across the different depths in the study area ranges from 11.30 **dScm^{-1}** to 56.97 **dScm^{-1}**. The lowest value was recorded at location C2, while the highest value was observed at location B3. These findings are supported by Table 3 and Figures 4e and 4f. It is worth noting that total dissolved solids (TDS) can serve as a proxy for electric conductivity.

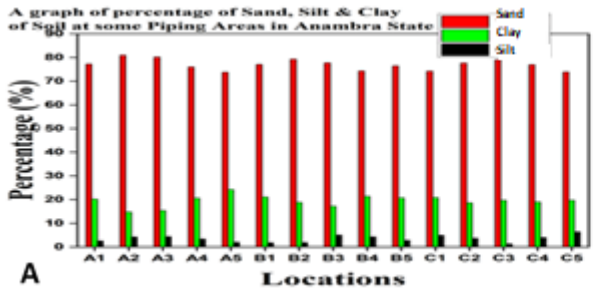
A graph of percentage of Sand, Silt & Clay of Soil at some Piping Areas in Anambra State
Sand
Clay
Silt
Percentage (%)
A1 A2 A3 A4 A5 B1 B2 B3 B4 B5 C1 C2 C3 C4 C5
Locations

A

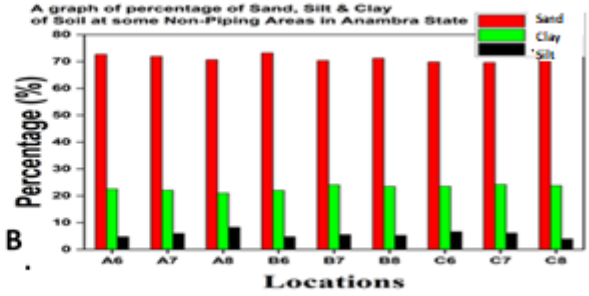
A graph of percentage of Sand, Silt & Clay of Soil at some Non-Piping Areas in Anambra State
Sand
Clay
Silt
Percentage (%)
A6 A7 A8 B6 B7 B8 C6 C7 C8
Locations

B

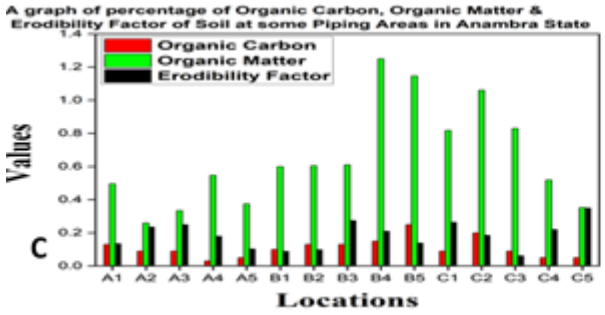
A graph of percentage of Organic Carbon, Organic Matter & Erodibility Factor of Soil at some Piping Areas in Anambra State
Organic Carbon
Organic Matter
Erodibility Factor
Values
A1 A2 A3 A4 A5 B1 B2 B3 B4 B5 C1 C2 C3 C4 C5
Locations

C

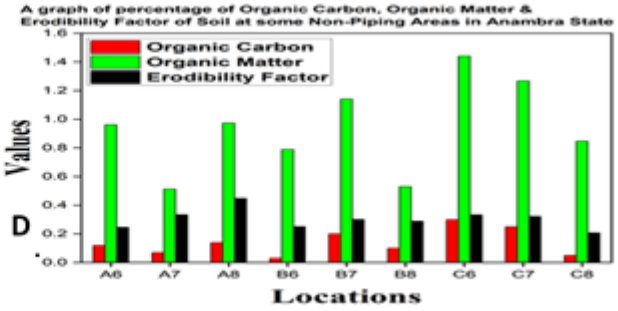
A graph of percentage of Organic Carbon, Organic Matter & Erodibility Factor of Soil at some Non-Piping Areas in Anambra State
Organic Carbon
Organic Matter
Erodibility Factor
Values
A6 A7 A8 B6 B7 B8 C6 C7 C8
Locations

D

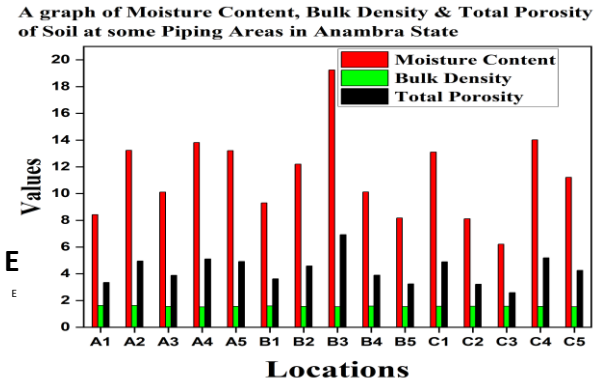
A graph of Moisture Content, Bulk Density & Total Porosity of Soil at some Piping Areas in Anambra State
Moisture Content
Bulk Density
Total Porosity
Values
A1 A2 A3 A4 A5 B1 B2 B3 B4 B5 C1 C2 C3 C4 C5
Locations

E

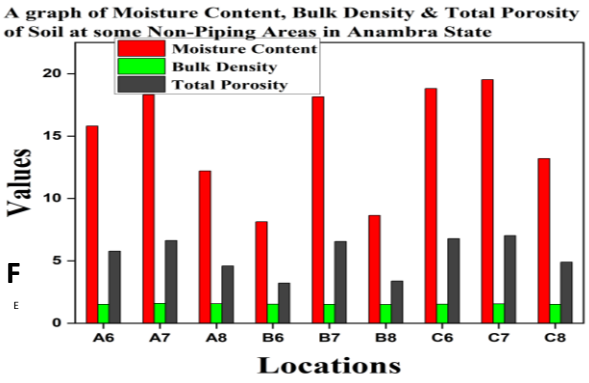
A graph of Moisture Content, Bulk Density & Total Porosity of Soil at some Non-Piping Areas in Anambra State
Moisture Content
Bulk Density
Total Porosity
Values
A6 A7 A8 B6 B7 B8 C6 C7 C8
Locations

F

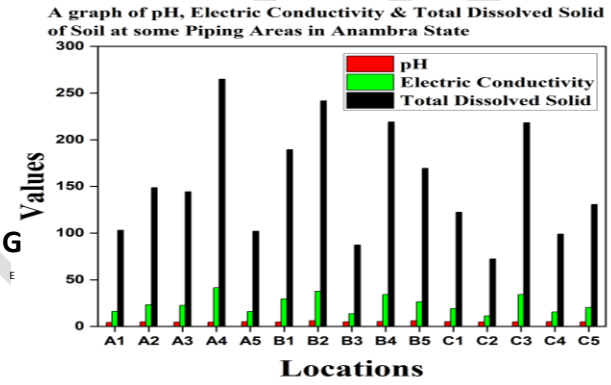
A graph of pH, Electric Conductivity & Total Dissolved Solid of Soil at some Piping Areas in Anambra State
pH
Electric Conductivity
Total Dissolved Solid
Values
A1 A2 A3 A4 A5 B1 B2 B3 B4 B5 C1 C2 C3 C4 C5
Locations

G

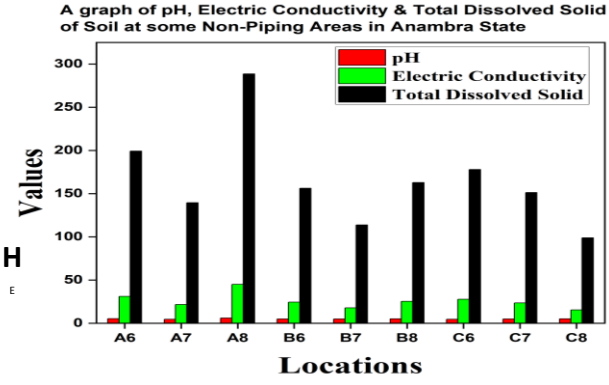
A graph of pH, Electric Conductivity & Total Dissolved Solid of Soil at some Non-Piping Areas in Anambra State
pH
Electric Conductivity
Total Dissolved Solid
Values
A6 A7 A8 B6 B7 B8 C6 C7 C8
Locations

H

Figure 4. (a) A graph soil texture at the piping area (b) A graph of soil texture at the non-piping area

(c) A graph of OM, OC and K_F at the piping area (d) A graph of OM, OC and K_F at the non-piping area

(e) A graph of MC, D_B and P_t at the piping area (f) A graph of MC, D_B and P_t at the non-piping area

(g) A graph of pH, EC and TDS at the piping area (h) A graph of pH, EC and TDS at the non-piping area

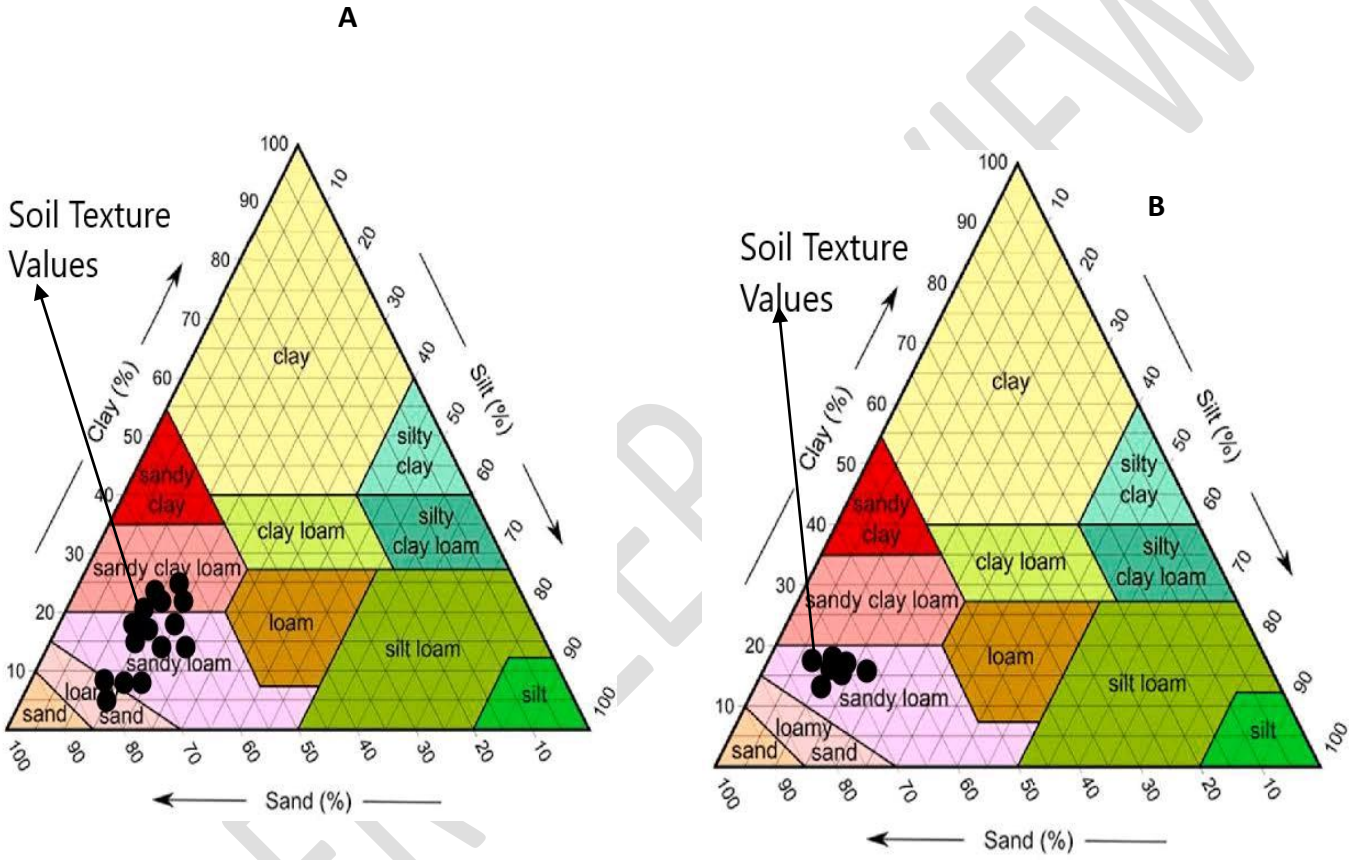

Figure 5. (a) Ternary graph for soil texture class at the piping area

(b) Ternary graph for soil texture class at the non-piping area

Table 3. Mean Values of soil texture at different Soil Depth

S/N	Code	Elevation	Latitude	Longitude	Sand (%) Soil Depth (ft.)				Clay (%) Soil Depth (ft.)				Silt (%) Soil Depth (ft.)				Remark
					0.5	1.5	2.5	Mean	0.5	1.5	2.5	Mean	0.5	1.5	2.5	Mean	
1	A1	212.9	6.1967	7.0959	85.2	72.3	74.2	77.2	14	23.6	23.1	20.2	0.8	4.1	2.7	2.5	SH
2	A2	216.3	6.1916	7.0936	80.4	83	79.5	81.0	15.9	14.1	14.4	14.8	3.7	2.9	6.1	4.2	PA
3	A3	218.2	6.1884	7.1028	81.3	78.1	81.2	80.2	18.5	17.5	10.2	15.4	0.2	4.4	8.6	4.4	PA
4	A4	209.8	6.2063	7.0936	79	74	75	76.0	19.2	22.3	20.4	20.6	1.8	3.7	4.6	3.4	PA
5	A5	210.1	6.2045	7.1055	72	70.3	79	73.8	25.2	27.4	20.1	24.2	2.8	2.3	0.9	2.0	PA
6	A6	229.9	6.1134	7.0577	70	75	73	72.7	23.2	22.1	22.4	22.6	6.8	2.9	4.6	4.8	NPA
7	A7	225.8	6.1217	7.0715	73.2	67.2	75.3	71.9	23.2	26.6	16.5	22.1	3.6	6.2	8.2	6.0	NPA
8	A8	216.8	6.1631	7.0623	69	70.1	73	70.7	22.5	20.1	20.4	21.0	8.5	9.8	6.6	8.3	NPA
9	B1	199	6.2261	7.0434	74	78	79.3	77.1	24.2	20.6	18.5	21.1	1.8	1.4	2.2	1.8	SH
10	B2	200.3	6.2367	7.0554	83.2	77.5	77.1	79.3	16.1	21.1	19.3	18.8	0.7	1.4	3.6	1.9	PA
11	B3	199.4	6.2362	7.0296	75	80.1	78.2	77.8	22.2	14.1	15.3	17.2	2.8	5.8	6.5	5.0	PA
12	B4	204.3	6.2192	7.0535	75.4	78.2	69.4	74.3	20.1	16.8	27.3	21.4	4.5	5	3.3	4.3	PA
13	B5	206.2	6.2137	7.0317	77.2	79	73.2	76.5	20.8	18.2	23.2	20.7	2	2.8	3.6	2.8	PA
14	B6	229.1	6.1562	7.0227	73	75.1	71.6	73.2	22.5	19.4	24.1	22.0	4.5	5.5	4.3	4.8	NPA
15	B7	227.1	6.1429	7.0319	69.2	75.6	66.3	70.4	24.1	22.1	26.1	24.1	6.7	2.3	7.6	5.5	NPA
16	B8	231.6	6.1351	7.0186	70.1	70.5	73.1	71.2	26.2	24.2	20.1	23.5	3.7	5.3	6.8	5.3	NPA
17	C1	237.1	6.0941	7.0241	70.2	77.4	75.1	74.2	22.1	20.1	20.3	20.8	7.7	2.5	4.6	4.9	SH
18	C2	238.2	6.0923	7.0223	83.2	70.5	79.3	77.7	12.5	24.2	19.2	18.6	4.3	5.3	1.5	3.7	PA
19	C3	230.1	6.0983	7.0204	88.5	74.5	74.1	79.0	11.2	23.7	24.2	19.7	0.3	1.8	1.7	1.3	PA
20	C4	242.1	6.0854	7.0315	79.2	75.4	76.4	77.0	19.5	19.3	18.2	19.0	1.3	5.3	5.4	4.0	PA
21	C5	244.4	6.0757	7.0191	75.2	69.3	77.2	73.9	19.2	27.1	12.9	19.7	5.6	3.6	9.9	6.4	PA
22	C6	240	6.1346	7.0001	70.1	68.3	71.2	69.9	22.1	26.4	22.1	23.5	7.8	5.3	6.7	6.6	NPA
23	C7	241.4	6.1024	6.9827	69	73.7	66.3	69.7	23.3	22.1	27.2	24.2	7.7	4.2	6.5	6.1	NPA
24	C8	241	6.0753	6.9933	70.1	67.5	79.1	72.2	23.1	28.1	20.2	23.8	6.8	4.4	0.7	4.0	NPA

Table 4. Mean Values of Organic Carbon, Organic Matter and Erodibility Factors at different Soil Depth

S/N	Code	Elevation	Latitude	Longitude	Organic Carbon (%) Soil Depth(ft)				Organic Matter (%) Soil Depth (ft)				Erodibility Factor Soil Depth (ft)				Remark
					0.5	1.5	2.5	Mean	0.5	1.5	2.5	Mean	0.5	1.5	2.5	Mean	
1	A1	212.9	6.1967	7.0959	0.51	0.22	0.13	0.29	0.88	0.38	0.22	0.50	0.03	0.23	0.15	0.13	SH
2	A2	216.3	6.1916	7.0936	0.22	0.14	0.09	0.15	0.38	0.24	0.16	0.26	0.20	0.15	0.35	0.23	PA
3	A3	218.2	6.1884	7.1028	0.31	0.18	0.09	0.19	0.54	0.31	0.16	0.33	0.01	0.25	0.49	0.25	PA
4	A4	209.8	6.2063	7.0936	0.62	0.3	0.03	0.32	1.07	0.52	0.05	0.55	0.08	0.20	0.26	0.18	PA
5	A5	210.1	6.2045	7.1055	0.42	0.18	0.05	0.22	0.73	0.31	0.09	0.37	0.14	0.13	0.04	0.10	PA
6	A6	229.9	6.1134	7.0577	1.34	0.21	0.12	0.56	2.32	0.36	0.21	0.96	0.34	0.15	0.25	0.25	NPA
7	A7	225.8	6.1217	7.0715	0.61	0.21	0.07	0.30	1.05	0.36	0.12	0.51	0.17	0.38	0.45	0.33	NPA
8	A8	216.8	6.1631	7.0623	1.02	0.53	0.14	0.56	1.76	0.92	0.24	0.97	0.43	0.55	0.36	0.45	NPA
9	B1	199	6.2261	7.0434	0.61	0.33	0.1	0.35	1.05	0.57	0.17	0.60	0.09	0.07	0.11	0.09	SH
10	B2	200.3	6.2367	7.0554	0.71	0.21	0.13	0.35	1.23	0.36	0.22	0.61	0.03	0.07	0.20	0.10	PA
11	B3	199.4	6.2362	7.0296	0.52	0.41	0.13	0.35	0.90	0.71	0.22	0.61	0.15	0.31	0.37	0.27	PA
12	B4	204.3	6.2192	7.0535	1.21	0.81	0.15	0.72	2.09	1.40	0.26	1.25	0.22	0.22	0.19	0.21	PA
13	B5	206.2	6.2137	7.0317	1.02	0.72	0.25	0.66	1.76	1.24	0.43	1.15	0.09	0.13	0.20	0.14	PA
14	B6	229.1	6.1562	7.0227	0.91	0.43	0.03	0.46	1.57	0.74	0.05	0.79	0.23	0.28	0.24	0.25	NPA
15	B7	227.1	6.1429	7.0319	1.08	0.7	0.2	0.66	1.87	1.21	0.35	1.14	0.35	0.10	0.45	0.30	NPA
16	B8	231.6	6.1351	7.0186	0.51	0.31	0.1	0.31	0.88	0.54	0.17	0.53	0.19	0.30	0.38	0.29	NPA
17	C1	237.1	6.0941	7.0241	1.12	0.21	0.09	0.47	1.94	0.36	0.16	0.82	0.41	0.13	0.25	0.26	SH
18	C2	238.2	6.0923	7.0223	1.21	0.43	0.2	0.61	2.09	0.74	0.35	1.06	0.17	0.31	0.07	0.18	PA
19	C3	230.1	6.0983	7.0204	0.84	0.51	0.09	0.48	1.45	0.88	0.16	0.83	0.01	0.08	0.09	0.06	PA
20	C4	242.1	6.0854	7.0315	0.63	0.22	0.05	0.30	1.09	0.38	0.09	0.52	0.06	0.30	0.31	0.22	PA
21	C5	244.4	6.0757	7.0191	0.41	0.15	0.05	0.20	0.71	0.26	0.09	0.35	0.28	0.21	0.55	0.35	PA
22	C6	240	6.1346	7.0001	1.31	0.89	0.3	0.83	2.26	1.54	0.52	1.44	0.36	0.27	0.37	0.33	NPA
23	C7	241.4	6.1024	6.9827	1.05	0.9	0.25	0.73	1.82	1.56	0.43	1.27	0.40	0.19	0.38	0.32	NPA
24	C8	241	6.0753	6.9933	0.9	0.52	0.05	0.49	1.56	0.90	0.09	0.85	0.33	0.26	0.03	0.21	NPA

Table 5. Mean Values of Moisture Content, Bulk Density and Total Porosity at different Soil Depth

S/N	Code	Elevation	Latitude	Longitude	Moisture Content (%) Soil Depth (ft)				Bulk Density (g/cm^3) Soil Depth (ft)				Total Porosity (%) Soil Depth (ft)				Remark
					0.5	1.5	2.5	Mean	0.5	1.5	2.5	Mean	0.5	1.5	2.5	Mean	
1	A1	212.9	6.1967	7.0959	1.71	3.22	8.42	4.45	1.72	1.63	1.55	1.63	33.85	37.31	40.38	37.18	SH
2	A2	216.3	6.1916	7.0936	2.65	8.22	13.23	8.03	1.73	1.62	1.53	1.63	33.46	37.69	41.15	37.44	PA
3	A3	218.2	6.1884	7.1028	4.71	10.11	10.11	8.31	1.66	1.54	1.48	1.56	36.15	40.77	43.08	40.00	PA
4	A4	209.8	6.2063	7.0936	4.12	5.11	13.82	7.68	1.51	1.56	1.50	1.52	41.92	40.00	42.31	41.41	PA
5	A5	210.1	6.2045	7.1055	1.18	8.11	13.21	7.50	1.62	1.54	1.50	1.55	37.69	40.77	42.31	40.26	PA
6	A6	229.9	6.1134	7.0577	4.61	12.21	15.81	10.88	1.52	1.54	1.49	1.52	41.54	40.77	42.69	41.67	NPA
7	A7	225.8	6.1217	7.0715	10.71	16.22	18.31	15.08	1.62	1.64	1.52	1.59	37.69	36.92	41.54	38.72	NPA
8	A8	216.8	6.1631	7.0623	11.71	10.20	12.21	11.37	1.65	1.54	1.50	1.56	36.54	40.77	42.31	39.87	NPA
9	B1	199	6.2261	7.0434	2.10	5.81	9.30	5.74	1.64	1.60	1.53	1.59	36.92	38.46	41.15	38.85	SH
10	B2	200.3	6.2367	7.0554	8.50	11.20	12.20	10.63	1.52	1.62	1.54	1.56	41.54	37.69	40.77	40.00	PA
11	B3	199.4	6.2362	7.0296	8.82	13.11	19.25	13.73	1.62	1.50	1.50	1.54	37.69	42.31	42.31	40.77	PA
12	B4	204.3	6.2192	7.0535	2.72	8.11	10.12	6.98	1.71	1.54	1.50	1.58	34.23	40.77	42.31	39.10	PA
13	B5	206.2	6.2137	7.0317	1.80	4.12	8.18	4.70	1.54	1.58	1.53	1.55	40.77	39.23	41.15	40.38	PA
14	B6	229.1	6.1562	7.0227	1.22	6.11	8.13	5.15	1.61	1.50	1.48	1.53	38.08	42.31	43.08	41.15	NPA
15	B7	227.1	6.1429	7.0319	9.71	13.11	18.15	13.66	1.52	1.52	1.50	1.51	41.54	41.54	42.31	41.79	NPA
16	B8	231.6	6.1351	7.0186	4.72	10.35	8.65	7.91	1.54	1.50	1.49	1.51	40.77	42.31	42.69	41.92	NPA
17	C1	237.1	6.0941	7.0241	1.28	2.05	13.11	5.48	1.71	1.52	1.50	1.58	34.23	41.54	42.31	39.36	SH
18	C2	238.2	6.0923	7.0223	3.01	11.21	8.11	7.44	1.61	1.57	1.53	1.57	38.08	39.62	41.15	39.62	PA
19	C3	230.1	6.0983	7.0204	1.30	1.11	6.21	2.87	1.71	1.52	1.50	1.58	34.23	41.54	42.31	39.36	PA
20	C4	242.1	6.0854	7.0315	3.71	3.11	14.02	6.95	1.51	1.62	1.56	1.56	41.92	37.69	40.00	39.87	PA
21	C5	244.4	6.0757	7.0191	1.48	6.32	11.22	6.34	1.52	1.58	1.52	1.54	41.54	39.23	41.54	40.77	PA
22	C6	240	6.1346	7.0001	5.31	11.22	18.81	11.78	1.54	1.58	1.49	1.54	40.77	39.23	42.69	40.90	NPA
23	C7	241.4	6.1024	6.9827	2.71	8.11	19.52	10.11	1.64	1.53	1.48	1.55	36.92	41.15	43.08	40.38	NPA
24	C8	241	6.0753	6.9933	9.40	4.31	13.20	8.97	1.52	1.52	1.50	1.51	41.54	41.54	42.31	41.79	NPA

Table 6. Mean Values of pH, Electric Conductivity and Total Dissolved Solid at different Soil Depth

S/N	Code	Elevation	Latitude	Longitude	pH				EC				TDS				Remark
					Soil Depth (ft)				Soil Depth (ft)				Soil Depth (ft)				
					0.5	1.5	2.5	Mean	0.5	1.5	2.5	Mean	0.5	1.5	2.5	Mean	
1	A1	212.9	6.1967	7.0959	4.1	4.8	4	4.3	22.1	15.2	11	16.10	141.44	97.28	70.4	103.04	SH
2	A2	216.3	6.1916	7.0936	4.8	5.4	4.7	5.0	45.1	12.6	12	23.23	288.64	80.64	76.8	148.69	PA
3	A3	218.2	6.1884	7.1028	7.1	7	7.1	7.1	31.5	23	13.1	22.53	201.6	147.2	83.84	144.21	PA
4	A4	209.8	6.2063	7.0936	6.8	6.7	6.6	6.7	62.1	41	21.1	41.40	397.44	262.4	135.04	264.96	PA
5	A5	210.1	6.2045	7.1055	5.1	5.6	4.7	5.1	21.2	26.5	0.1	15.93	135.68	169.6	0.64	101.97	PA
6	A6	229.9	6.1134	7.0577	5.8	5.1	5.2	5.4	52.1	31.1	10.2	31.13	333.44	199.04	65.28	199.25	NPA
7	A7	225.8	6.1217	7.0715	5.5	6.9	5.7	6.0	32.1	23.1	10.2	21.80	205.44	147.84	65.28	139.52	NPA
8	A8	216.8	6.1631	7.0623	7.2	7.2	7.2	7.2	52.1	51.1	32.1	45.10	333.44	327.04	205.44	288.64	NPA
9	B1	199	6.2261	7.0434	4.1	5.2	5	4.8	41.5	32.1	15.2	29.60	265.6	205.44	97.28	189.44	SH
10	B2	200.3	6.2367	7.0554	6.4	6.6	5.8	6.3	61.1	30.7	21.5	37.77	391.04	196.48	137.6	241.71	PA
11	B3	199.4	6.2362	7.0296	5.9	5.4	5.7	5.7	21.2	5.6	14.1	13.63	135.68	35.84	90.24	87.25	PA
12	B4	204.3	6.2192	7.0535	6.1	6.6	5.9	6.2	51	37.2	14.5	34.23	326.4	238.08	92.8	219.09	PA
13	B5	206.2	6.2137	7.0317	6.3	5.8	6.3	6.1	32.1	38.2	9.1	26.47	205.44	244.48	58.24	169.39	PA
14	B6	229.1	6.1562	7.0227	6.8	6.8	6.7	6.8	41.1	20.1	12.1	24.43	263.04	128.64	77.44	156.37	NPA
15	B7	227.1	6.1429	7.0319	4.8	5.5	4.5	4.9	21.1	21.1	11.2	17.80	135.04	135.04	71.68	113.92	NPA
16	B8	231.6	6.1351	7.0186	5.2	5.1	5.2	5.2	31.2	25.1	20.1	25.47	199.68	160.64	128.64	162.99	NPA
17	C1	237.1	6.0941	7.0241	4.8	5.4	5.1	5.1	20.1	24.1	13.2	19.13	128.64	154.24	84.48	122.45	SH
18	C2	238.2	6.0923	7.0223	4.9	4.9	4.6	4.8	15.6	8.2	10.1	11.30	99.84	52.48	64.64	72.32	PA
19	C3	230.1	6.0983	7.0204	5.5	5.3	4.2	5.0	52.1	36.1	14.1	34.10	333.44	231.04	90.24	218.24	PA
20	C4	242.1	6.0854	7.0315	7.1	6.9	6.9	7.0	25.1	20.1	1.2	15.47	160.64	128.64	7.68	98.99	PA
21	C5	244.4	6.0757	7.0191	6.5	6.3	6	6.3	28.1	13.1	20.1	20.43	179.84	83.84	128.64	130.77	PA
22	C6	240	6.1346	7.0001	4.9	4.7	4.4	4.7	32.1	41.2	10.1	27.80	205.44	263.68	64.64	177.92	NPA
23	C7	241.4	6.1024	6.9827	4.9	5.2	5.1	5.1	29.6	30.1	11.2	23.63	189.44	192.64	71.68	151.25	NPA
24	C8	241	6.0753	6.9933	5.1	5.1	5.2	5.1	11.2	26.1	9.1	15.47	71.68	167.04	58.24	98.99	NPA

Discussion

The soils within the study area exhibit a predominantly sandy composition, which demonstrates a decreasing trend with increasing depth, as indicated in Table 3. This characteristic can be attributed to the study area's proximity to the origin of Nanka sands. These sands originate from the Imo shale, a shale unit that derives from a coastal sandy mudstone. Notably, the Nanka sands are well-known for their distinct porous structure, which composed of coarse-grained and pebbly quartz sands. The relatively low presence of silt and clay soils may be attributed to the soil's susceptibility to leaching, which occurs in the Nanka sandy zones. The leaching process contributes to the unstable nature of the soil in these areas [47].

By analyzing Figure 4a and 4b, it becomes apparent that the soil composition near the sinkhole structure exhibits a higher proportion of sandy soil and a lower proportion of clayey soil compared to areas located further away (e.g., B1, B2, and C2). This observation can be explained by the process of dispersion, which reduces infiltration and leads to water runoff. Consequently, fine particles are carried and deposited, exacerbating the formation of soil piping. As a result, areas in close proximity to erosion sites typically exhibit higher levels of sand content and increased porosity. This result is consonance with the works of [22], [32].

The relatively low presence of organic carbon in the study area can be attributed to various factors, encompassing both natural processes and human activities. Sheet erosion and leaching of the soil contribute to the dispersal of organic matter, resulting in its reduced quantity. Additionally, the rapid expansion of urban structures leads to a significant reduction in soil vegetative cover, further exacerbating the decline in organic matter levels.

The aforementioned removal of vegetation can also be linked to the diminished values of organic carbon. This removal potentially causes the loss of nitrates within the soil, thus negatively affecting the organic matter content. According to the work of [54], soils with organic matter lesser than 2% are at their critical level, while [55] opined that are less than 3.5% organic carbon content can be considered erodible.

When examining the distribution of organic carbon (OC) and organic matter (OM) based on the values presented in Table 4, it becomes evident that there is no discernible pattern or order. Both low and extreme low values of OC and OM are observed in areas affected by soil piping as well as non-piping areas across different regions, these result obtained is similar to the works [37], [56].

Moisture content, representing the amount of water present in the soil, serves as a valuable indicator of the soil's responses to erosion and soil loss. Extremes in moisture content, whether high or low are typically associated with higher erosion rates. Conversely, intermediate moisture levels tend to exhibit greater resistance to erosion, particularly for soils comprised of finer particles. However, for coarse-grained soils, moisture content can have a negative impact on erosion resistance. Previous studies have determined that a moisture content range of 22% to 24% is desirable for heavy loamy soils [1], [57]. However, the observed moisture contents in the study area, especially in regions close to soil piping areas, are generally low, as indicated in table 5, which is similar to the work of [57], in Nnewi, Anambra state . This may explain the recurring instances of gully erosion and soil piping documented in the state.

Bulk density, a parameter commonly employed to assess soil compaction, is determined by the ratio of soil weight to the combined volume of soil particles and the voids between them. A bulk density value greater than 1.4 g/cm^3 indicates low soil porosity and compaction [37]. The diminished presence of air and water movement through the soil resulting from these low values can significantly reduce fluid permeability. Consequently, runoff, soil loss, and erosion are more likely to occur on sloping land.

Table 5 highlights the highest bulk density value of 1.63 g/cm^3 found in area A1, a region characterized by soil piping, while the lowest total porosity value of 41.92 % is recorded in area B8, a non-piping area.

The pH level of soil serves as an indicator of its acidity or alkalinity. Soils that contain high levels of salt tend to have an elevated pH value. Sodicity in soil refers to the presence of higher sodium (Na+) content, while the levels of other ions

such as H+, Al+, Mg+, and K+ are relatively low [25]. Consequently, sodic soils exhibit a significant alteration in the plasticity of clay minerals, leading to dispersion and swelling [30], [35]. These changes often result in poor soil structure and reduced infiltration rates.

In the study areas, where the topsoil consists of sand and the subsoil is composed of dense clay, sodicity in the soil is commonly observed. This combination of soil types contributes to the favorability of sodicity. As a result, the pH range and distribution shift from slightly acidic to alkaline conditions.

Table 6 indicates that the soils surrounding areas A4, A3, A8, B6, C4, and C5 exhibit the highest pH values. These soils are known to have high salt content, which promotes dispersion and sealing. Consequently, water runoff may occur in these areas, leading to the diffusion of water towards regions with slightly acidic conditions. The acidity of these regions may conduct water into the ground abnormally (increasing the velocity of infiltration). This process may erode the soil and cause soil piping.

Soil salinity is often described using parameters such as electric conductivity (EC) and total dissolved solids (TDS). EC is a measure of the soil's ability to conduct electric current[58]. This conductivity depends on factors such as the total concentration of dissolved ions, the ionic strength, and the temperature of the soil. As water is known to conduct electric current, EC values are commonly used to assess the velocity of water infiltration in the soil. Higher EC values indicate a greater flow of water through the soil's pore spaces [58].

Soils with high sandy content, high porosity and low compaction tend to exhibit higher EC values [25]. These soil characteristics have been found to be positively associated with erosion occurrence. While TDS, on the other hand, represents the total concentration of dissolved ions in the soil and is commonly used as an indicator of the soil's salt content [4], [32], [58]. While the relationship between EC and TDS is not always linear, a strong correlation exists between the two, as noted by [58]. This correlation is significantly influenced by the salinity content of the soil.

Analyzing the investigation's findings, it is evident that the distribution of EC and TDS throughout the study area ranges from low to moderate values. Table 6 highlights that areas A1, A2, B2, B3, B7, and C3 recorded the highest EC and TDS values. Conversely, areas A3, C2, and C4 exhibited the lowest values.

Conclusion

The findings unveiled a range of soil acidity, varying from slightly acidic to alkaline, within the study areas. Moreover, it was observed that the soil exhibited poor clayey content and high porosity, resulting in increased sodicity, dispersion, and sealing. Consequently, these factors have contributed to inadequate infiltration and heightened runoff. The discussion further indicates that the prevalence of various forms of erosion within the state can be attributed to the elevated rate of runoff and unfavorable soil conditions, which have consequently led to the occurrence of sinkholes and soil subsidence.

In light of these findings, it is imperative to encourage further research aimed at addressing and ameliorating the state's soil conditions. To facilitate this, it is crucial for the government and other stakeholders to allocate financial resources for grants, thereby fostering the advancement of knowledge in this crucial field.

Reference

[1] R. Green, “Infiltration of water into soils as influenced by antecedent moisture,” Jan. 1962, Accessed: Aug. 25, 2023. [Online]. Available: https://dr.lib.iastate.edu/handle/20.500.12876/73601

[2] W. Ma, X. Zhang, Q. Zhen, and Y. Zhang, “Effect of soil texture on water infiltration in semiarid reclaimed land,” *Water Quality Research Journal*, vol. 51, no. 1, pp. 33–41, Feb. 2016, doi: 10.2166/wqrjc.2015.025.

[3] R. Parihar, S. Kumar, V. Kumar, and S. Swami, “Factors Affecting Infiltration and its Management Strategies,” 2023.

[4] A. A. Ameloko and E. A. Ayolabi, “Geophysical assessment for vertical leachate migration profile and physicochemical study of groundwater around the Olusosun dumpsite Lagos, south-west Nigeria,” *Appl Water Sci*, vol. 8, no. 5, p. 142, Aug. 2018, doi: 10.1007/s13201-018-0775-x.

[5] R. Pan, A. Martinez, T. Brito, and E. Seidel, “Processes of Soil Infiltration and Water Retention and Strategies to Increase Their Capacity,” *Journal of Experimental Agriculture International*, vol. 20, pp. 1–14, Jan. 2018, doi: 10.9734/JEAI/2018/39132.
[6] T. Zhang and G. V. Wilson, “Spatial distribution of pipe collapses in Goodwin Creek Watershed, Mississippi: SPATIAL DISTRIBUTION OF PIPE COLLAPSES,” *Hydrol. Process.*, vol. 27, no. 14, pp. 2032–2040, Jul. 2013, doi: 10.1002/hyp.9357.
[7] F. Cleophas *et al.*, “Effect of soil physical properties on soil infiltration rates,” *J. Phys.: Conf. Ser.*, vol. 2314, no. 1, p. 012020, Aug. 2022, doi: 10.1088/1742-6596/2314/1/012020.
[8] E. Babur *et al.*, “Studying soil erosion by evaluating changes in physico-chemical properties of soils under different land-use types,” *Journal of the Saudi Society of Agricultural Sciences*, vol. 20, no. 3, pp. 190–197, Apr. 2021, doi: 10.1016/j.jssas.2021.01.005.
[9] P. O. Phil-Eze, “Variability of soil properties related to vegetation cover in a tropical rainforest landscape,” *Journal of Geography and Regional Planning*, vol. 3, pp. 177–184, 2010.
[10] A. Bernatek-Jakiel and M. Kondracka, “Combining geomorphological mapping and near surface geophysics (GPR and ERT) to study piping systems,” *Geomorphology*, vol. 274, pp. 193–209, Dec. 2016, doi: 10.1016/j.geomorph.2016.09.018.
[11] C. Castañeda *et al.*, “Origin and evolution of Sariñena Lake (central Ebro Basin): A piping-based model,” *Geomorphology*, vol. 290, pp. 164–183, Aug. 2017, doi: 10.1016/j.geomorph.2017.04.013.
[12] I. U. Chibuogwu and G. Z. Ugwu, “An Open Investigation of Some Soil Pipes Forming Soil Subsidence at Awka South Local Government Area Using Very Low Frequency Electromagnetic Geophysical Technique,” *International Journal of Scientific Research in Multidisciplinary Studies*, vol. 9, no. 2, pp. 40–45, 2023.
[13] M. Joshi *et al.*, “Detection of soil pipes through remote sensing and electrical resistivity method: Insight from southern Western Ghats, India,” *Quaternary International*, vol. 575–576, pp. 51–61, Feb. 2021, doi: 10.1016/j.quaint.2020.08.021.
[14] A. Bernatek-Jakiel, M. Jakiel, and K. Krzemień, “Piping dynamics in mid-altitude mountains under a temperate climate: Bieszczady Mountains, eastern Carpathians: PIPING DYNAMICS: EROSION RATES AND PIPE ELONGATION,” *Earth Surf. Process. Landforms*, vol. 42, no. 9, pp. 1419–1433, Jul. 2017, doi: 10.1002/esp.4160.
[15] A. Bernatek-Jakiel and J. Poesen, “Subsurface erosion by soil piping: significance and research needs,” *Earth-Science Reviews*, vol. 185, pp. 1107–1128, Oct. 2018, doi: 10.1016/j.earscirev.2018.08.006.
[16] J. M. García-Ruiz, S. Beguería, N. Lana-Renault, E. Nadal-Romero, and A. Cerdà, “Ongoing and Emerging Questions in Water Erosion Studies,” *Land Degrad. Develop.*, vol. 28, no. 1, pp. 5–21, Jan. 2017, doi: 10.1002/ldr.2641.
[17] R. B. Bryan and J. A. A. Jones, “The significance of soil piping processes: inventory and prospect,” *Geomorphology*, vol. 20, no. 3–4, pp. 209–218, Oct. 1997, doi: 10.1016/S0169-555X(97)00024-X.
[18] E. Nadal-Romero, E. Verachtert, R. Maes, and J. Poesen, “Quantitative assessment of the piping erosion susceptibility of loess-derived soil horizons using the pinhole test,” *Geomorphology*, vol. 135, no. 1–2, pp. 66–79, Dec. 2011, doi: 10.1016/j.geomorph.2011.07.026.
[19] P. J. Hughes, “Tunnel erosion in the loess of Banks Peninsula,” 1970, doi: 10.26021/7937.
[20] R. B. Bryan and L. E. Harvey, “Observations on the Geomorphic Significance of Tunnel Erosion in a Semi-Arid Ephemeral Drainage System,” *Geografiska Annaler. Series A, Physical Geography*, vol. 67, no. 3/4, p. 257, 1985, doi: 10.2307/521103.
[21] J. A. A. Jones, J. M. Richardson, and H. J. Jacob, “Factors controlling the distribution of piping in Britain: a reconnaissance,” *Geomorphology*, vol. 20, no. 3–4, pp. 289–306, Oct. 1997, doi: 10.1016/S0169-555X(97)00030-5.
[22] M. Hardie, *Dispersive soils and their management*. Technical Reference Manual, 2009.
[23] M. G. Anderson, “Book reviews: Jones, J.A.A. 1981: The nature of soil piping - a review of research. BGRG Re search Monograph 3. Norwich: Geo Books. xiv + 301 pp. £12.40,” *Progress in Physical Geography: Earth and Environment*, vol. 7, no. 4, pp. 611–612, Dec. 1983, doi: 10.1177/030913338300700406.
[24] K. V. Sarath, S. E., D. .V, S.Gurudeth, and C. S. SubeeshChandran, *Subsurface erosion by soil piping: A case study from Adoor-Pandi Area, Kasaragod, Kerala, India*. 2020.

[25] "Research on Soil Piping – Kerala State Disaster Management Authority." https://sdma.kerala.gov.in/research-on-soil-piping/ (accessed Aug. 28, 2023).
[26] I. U. Chibuogwu and G. Z. Ugwu, "Chemical Analysis of Uncontrolled Soil Pipes Leading to Soil Subsidence in Anambra State Nigeria," *International Journal of Scientific Research in Multidisciplinary Studies*, vol. 9, no. 1, pp. 40–45, 2023.
[27] T. X. Zhu, "Deep-seated., complex tunnel systems — a hydrological study in a semi-arid catchment, Loess Plateau, China," *Geomorphology*, vol. 20, no. 3, pp. 255–267, Oct. 1997, doi: 10.1016/S0169-555X(97)00027-5.
[28] D. Norton, I. Shainberg, and L. Cihacek, "Erosion and Soil Chemical Properties," 1999, pp. 39–56.
[29] M. A. Nearing, S. Yin, P. Borrelli, and V. O. Polyakov, "Rainfall erosivity: An historical review," *CATENA*, vol. 157, pp. 357–362, Oct. 2017, doi: 10.1016/j.catena.2017.06.004.
[30] R. W. Fitzpatrick, S. C. Boucher, R. Naidu, and E. Fritsch, "Environmental consequences of soil sodicity," *Soil Res.*, vol. 32, no. 5, pp. 1069–1093, 1994, doi: 10.1071/sr9941069.
[31] C. A. Vacher, R. Loch, and S. R. Raine, "Identification and management of dispersive mine spoils," Jan. 01, 2004. http://www.acmer.com.au/research/attachments/DispersivespoilsreportfinalJune2004R.pdf (accessed Aug. 28, 2023).
[32] C. H. Okeke, K. I. Ubaoji, and F. C. Uzodinma, "Interaction of Chemical, Physicochemical and Geotechnical Soil Properties of Anambra State Gully Erosion Site," *Saudi Journal of Civil Engineering*, vol. 5, no. 10, pp. 379–390, 2021.
[33] R. J. Crouch, J. W. McGarity, and R. R. Storrier, "Tunnel formation processes in the Riverina area of N.S.W., Australia," *Earth Surface Processes and Landforms*, vol. 11, no. 2, pp. 157–168, 1986, doi: 10.1002/esp.3290110206.
[34] C. J. Rosewell, "Investigations into the control of earthwork tunnelling," *Journal of the Soil Conservation Service of New South Wales*, vol. 26, pp. 188–203, 1970.
[35] M. A. Hardie, W. E. Cotching, and P. R. Zund, "Rehabilitation of field tunnel erosion using techniques developed for construction with dispersive soils," *Soil Res.*, vol. 45, no. 4, p. 280, 2007, doi: 10.1071/SR06154.
[36] S. K. Carey and M.-K. Woo, "The role of soil pipes as a slope runoff mechanism, Subarctic Yukon, Canada," *Journal of Hydrology*, vol. 233, no. 1, pp. 206–222, Jun. 2000, doi: 10.1016/S0022-1694(00)00234-1.
[37] U. Ayadiuno and C. Ndulue Dominic, "An Investigation into some Soil Indices as Indicator of High Soil Erodibility in Anambra State, Southeastern, Nigeria," *International Journal of Modern Agriculture*, vol. 10, no. 2, pp. 3451–3464, 2021.
[38] R. U. Ayadiuno, D. C. Ndulue, C. C. Ndichie, A. T. Mozie, P. O. Phil-Eze, and A. C. Onyekwelu, "Geospatial Analysis of Soil Erosion Susceptibility and Causative Factors in Anambra State, South East, Nigeria," *SR*, no. 81, pp. 5–32, Dec. 2021, doi: 10.32861/sr.81.5.32.
[39] E. Ezenkwen, "Gully Erosion in Anambra State: Nnaka," *Patrotic Union Journal*, vol. 1, pp. 9–18, 2010.
[40] O. Nich and C. J. Okeke-Ogbu, "Erosion Problems and their impact in Anambra State, Nigeria (A case study of Nnaka Community)," *International Journal of Environment and Pollution Research*, vol. 5, pp. 24–87, 2017.
[41] A. Shakrudeen, A. Abiodun, I. Nkechi, and A. A. Olubumma, "Land Susceptibility to Soil Erosion in Orashi Catchment, Nnewi South, Anambra State Nigeria," *Proceedings of the International Association of Hydrological Sciences*, vol. 376, pp. 87–97, 2018.
[42] E. A. Uboh, W. N. Akhionbare, E. Oweremadu, and O. A. Onifade, "Characterization of soil Quality in Erosion Prone Environment of Ukpor, Nnewi-South L.G.A of Anambra Stat, Nigeria," *International Journal of Advances in Applied Science*, vol. Vol.2, no. 1, pp. 1–8, 2013.
[43] A. Ocheli, O. B. Ogbe, and G. O. Aigbadon, "Geology and geotechnical investigations of part of the Anambra Basin, Southeastern Nigeria: implication for gully erosion hazards," *Environ Syst Res*, vol. 10, no. 1, p. 23, Dec. 2021, doi: 10.1186/s40068-021-00228-2.
[44] I. U. Chibuogwu and G. Z. Ugwu, "Uncovering soil piping vulnerability using direct current geophysical techniques in Awka, Anambra State, Nigeria," *IJMRGE*, vol. 4, no. 3, pp. 426–450, 2023, doi: 10.54660/.IJMRGE.2023.4.3.426-450.

[45] O.-B. Ao and A. I.M., “Palynological evidence of the oldest (Albian) sediment in the Anambra Basin, Southeastrn Nigeria.,” *Journal of Biological and Chemical Research*, vol. Vol. 30, pp. 387–408, Jan. 2013.
[46] O. Adeigbe and E. Salufu, “Geology and depositional environment of Campano-Maastrichtian sediments in the Anambra Basin, Southeastern Nigeria: Evidence from field relationship and sedimentological study,” *Earth Sciences Research Journal*, vol. 13, pp. 148–165, Dec. 2009.
[47] “Provenance and tectonic setting of the Eocene Nanka Sandstone, Anambra Basin, Nigeria: Transactions of the Royal Society of South Africa: Vol 75, No 1.” https://www.tandfonline.com/doi/abs/10.1080/0035919X.2019.1682081 (accessed Aug. 25, 2023).
[48] C. P. Nzoiwu, E. I. Agulue, S. Mbah, and C. P. Igboanugo, “Impact of Land Use/Land Cover Change on Surface Temperature Condition of Awka Town, Nigeria,” *JGIS*, vol. 09, no. 06, pp. 763–776, 2017, doi: 10.4236/jgis.2017.96047.
[49] I. U. Chibuogwu and T. N. Obiekezie, “Solar Forcing on Meteorological Parameter in Nigeria,” *International Journal of Multidisciplinary Sciences and Advanced Technology*, vol. 2, no. 11, pp. 15–23, 2021.
[50] USEPA, “USEPA Document.” U.S Environmental Protection Agency, 2021.
[51] A. Ekpo, L. Orakwe, N. Tom-Cyprain, C. Umobi, and J. Maduegbuna, “Physico-chemical properties of soils derived from different geologic formations in typical rainfall agro-ecological zone,” *Poljoprivredna tehnika*, vol. 48, no. 1, pp. 16–27, 2023, doi: 10.5937/PoljTeh2301016E.
[52] C. Njoku, “Soil physico-chemical properties as affected by flood and erosion in Abakalilki, Southeastern, Nigeria,” *Asian J Agric & Biol*, vol. 6, no. 3, pp. 321–326, 2018.
[53] Wischmeier, W.H. and Smith, D.D, *Predicting Rainfall Erosion Losses*. The USDA Agricultural Handbook No. 537, Maryland, 1978.
[54] W. D. Kemper and E. J. Koch, *Aggregate Stability of Soils from Western United States and Canada: Measurement Procedure, Correlations with Soil Constituents*. Agricultural Research Service, U.S. Department of Agriculture, 1966.
[55] C. Emeh and O. Igwe, “Effect of environmental pollution on susceptibility of sesquioxide-rich soils to water erosion,” *Geology, Ecology, and Landscapes*, vol. 2, no. 2, pp. 115–126, Apr. 2018, doi: 10.1080/24749508.2018.1452484.
[56] R. Udegbunam Ayadiuno, “Analysis of Soil Erosion Causative Factors and Susceptibility in Anambra State, Southeastern, Nigeria,” *Biosc Biotech Res Comm*, vol. 14, no. 9, pp. 212–218, Sep. 2021, doi: 10.21786/bbrc/14.9.40.
[57] P. O. Akannam and S. E. Kakulu, “Industrial Impact On Selected Heavy Metals In Soils Of Nnewi-North Local Government Area, Anambra State, Southeast Nigeria | Semantic Scholar.” https://www.semanticscholar.org/paper/Industrial-Impact-On-Selected-Heavy-Metals-In-Soils-P.O-S.E/66d8672f3777a0277a10b3299ab879d9e0aa2ab3 (accessed Aug. 29, 2023).
[58] A. F. Rusydi, “Correlation between conductivity and total dissolved solid in various type of water: A review,” *IOP Conf. Ser.: Earth Environ. Sci.*, vol. 118, p. 012019, Feb. 2018, doi: 10.1088/1755-1315/118/1/012019.